HKIE THE HONG KONG INSTITUTION OF ENGINEERS 香港工程師學會

# Elementary process analysis of charge transfer processes of lithium-ion batteries through the distribution of relaxation times method

**Sohei Tomita, Daiki Kawaguchi, Satoshi Hirayama and Yoshitaka Inui**
Department of Electronic Systems Engineering, The University of Shiga Prefecture, Japan

## ABSTRACT

Electrochemical impedance spectra were analysed for laminated and commercially available cylindrical batteries with varying electrode materials and degrees of cycle degradation. The distribution of relaxation times method was used to isolate the elementary processes, enabling an investigation into how cathode materials and cycle degradation impact battery impedance. It was observed that batteries, irrespective of their cathode material, exhibited four impedance components within the frequency range of the charge transfer process, with distinctions in the charge transfer process of the cathode manifesting at lower frequencies. The consistent presence of four primary impedance components was also noted in batteries subjected to varying degradation cycles. The results indicate that the number of significant elementary processes within the battery remains unchanged across different cathode materials and degrees of cycle degradation. The observed increase in the electrochemical impedance owing to degradation was ascribed to the charge transfer process originating from the cathode material.

**KEYWORDS** Lithium-ion battery; electrochemical impedance spectroscopy; charge transfer impedance; cathode material; degradation
**CONTACT** Sohei Tomita oe23stomita@ec.usp.ac.jp
Received 27 February 2024

## 1. Introduction

Lithium-ion batteries are extensively used in electronic devices such as smartphones and personal computers owing to their high energy density and electromotive force. Recently, increasing attention has been directed towards their potential as driving power sources for electric vehicles (Sun et al., 2020).

The demands for high-performance batteries have spurred the development of several cathode and anode materials (Li et al., 2020). Historically, lithium cobalt oxide and nickel manganese cobalt oxide (NMC) were predominantly used as cathode materials in lithium-ion batteries. However, recently, nickel-rich NMC and lithium nickel cobalt aluminium oxide (NCA) have gained interest due to their potential to achieve a higher capacity (Zeng et al., 2018). To foster the widespread adoption of electric vehicles powered using lithium-ion batteries, it is imperative to enhance batteries' energy and power density (Ohzuku and Brodd, 2007). Moreover, the establishment of accurate prediction and simulation techniques for battery performance is crucial for the safe and sophisticated control of lithium-ion batteries. A notable challenge of lithium-ion batteries is the increase in their internal impedance due to degradation triggered by charge–discharge cycles (Okada et al., 2013).

In this study, the influence of different cathode materials on the internal impedance spectra of lithium-ion batteries was explored through measurements of lithium-ion batteries equipped with the NCA or NMC cathode material. In addition, the effect of cycle degradation on the internal impedance spectra was assessed by measuring the NMC cathode batteries subjected to various degradation cycles. The electrochemical impedance was gauged in accordance with the electrochemical impedance spectroscopy (EIS), followed by the application of the distribution of relaxation times (DRT) analysis (Illig et al., 2012) to examine the internal elementary processes of the battery cell.

## 2. Electrochemical impedance

EIS analysis is a non-invasive measurement technique frequently used for characterising the internal impedance of batteries (Choi et al., 2020). The frequency characteristics of the internal impedance of a battery is called electrochemical impedance, which can be obtained by applying a small sinusoidal alternating current or voltage to the battery and repeatedly measuring the voltage or current response while varying the frequency. The measured impedance is depicted using a graph known as the Nyquist plot. Figure 1 is an example of the electrochemical impedance of a lithium-ion battery represented by the Nyquist plot. The Nyquist plot features the real part of the impedance on the horizontal axis and the imaginary part of the impedance on the inverted vertical axis. Regarding lithium-ion batteries, the Nyquist plot of electrochemical impedance is categorised into three components: (a) Ohmic resistance; (b) charge transfer process; and (c) diffusion process. EIS is advantageous for characterising each internal resistance component. The lithium ions in the electrolyte turn into lithium at the electrode and vice versa by receiving and giving electrons on the electrode surface, which is called the charge transfer process (Jow et al., 2020). The charge transfer resistance

is linked to the kinetics of electrochemical reactions and the nature of the solid electrolyte interphase, and its characteristics are influenced by electrode materials and cycle degradation. Herein, we predominantly focus on the charge transfer process amongst the three components mentioned.

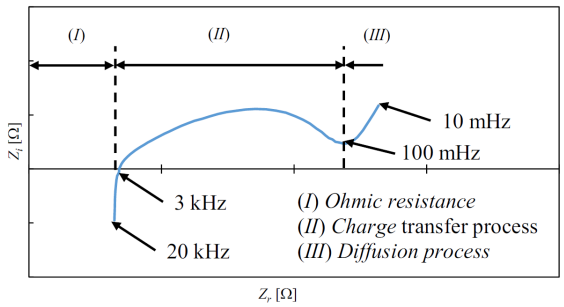


Figure 1. Example of the electrochemical impedance of a lithium-ion battery represented by the Nyquist plot.

### *2.1. Test batteries*

This study explored laminated lithium-ion batteries (manufactured by JFE Techno-Research, cell size 56 mm × 56 mm) and commercial cylindrical 18650 lithium-ion batteries (manufactured by Panasonic, diameter of 18 mm and height of 65 mm). Both battery types incorporate NCA or NMC cathodes and graphite anodes.

Degradation tests were conducted on commercial 18650 lithium-ion batteries equipped with a NMC cathode. In this study, these unused batteries were degraded by repetitive charging and discharging at 25 ºC using a battery test system (Kikusui Electronics Industry, PFX2011). The constant current and constant voltage (CC-CV) method was used for battery charging, whereas the CC method was used for discharging. During CC-CV charging, batteries were charged at a constant current of 2.2 A until the terminal voltage reached 4.2 V, followed by constant-voltage charging at 4.2 V for 3 h to achieve a fully charged state (state of charge [SOC] = 1.0). Post the CC-CV charging, the fully charged batteries were discharged at a constant current of 2.2 A until the terminal voltage decreased below the discharge cut-off voltage of 2.7 V, enabling the batteries to reach a fully discharged state (SOC = 0). Four degraded batteries were prepared by executing 50, 100, 150, and 200 degradation cycles, respectively. The discharge capacities of each degraded battery are provided in Table 1.

Table 1. Discharge capacities of each degraded battery.

| Number of cycles | Discharge capacity [mAh] |
|---|---|
| 0 | Nearly 2260 |
| 50 | 2183 |
| 100 | 2158 |
| 150 | 2130 |
| 200 | 2062 |

### *2.2. Measurement of electrochemical impedance*

The temperature of each test battery was maintained constant by placing it in a thermostatic chamber (ESPEC LU-124). The electrochemical impedance was measured within the frequency range from 10 mHz to 20 kHz using an potentio/galvanostat integrated FRA (Solartron 1280Z). Measurements were conducted under seven SOC conditions, ranging from 0.3 to 0.9 at intervals of 0.1 and four battery temperature conditions of -10 ºC, -5 ºC, 0 ºC, and 10 ºC.

Figure 2 illustrates the electrochemical impedances of two unused laminated batteries with either an NCA or NMC cathode alongside an unused commercial 18650 NCA battery at -10 ºC and an SOC of 0.8. When comparing the two types of laminated batteries, a significant difference in internal impedance is observed at frequencies below 10 Hz. A large arc manifests in the NCA cathode battery, a feature not present in the NMC cathode battery within the frequencies below 10 Hz. As both batteries share an identical material composition, except for the cathode, this variance in internal impedance is attributed to the cathode. Conversely, upon comparing the measurement outcomes of the two NCA battery types, their qualitative characteristics are analogous in that impedance escalates linearly on the high-frequency side and a large arc emerges on the low-frequency side, albeit with differing magnitudes. These results indicate that the disparity in cathode materials is chiefly exhibited in the internal impedance on the low-frequency side.

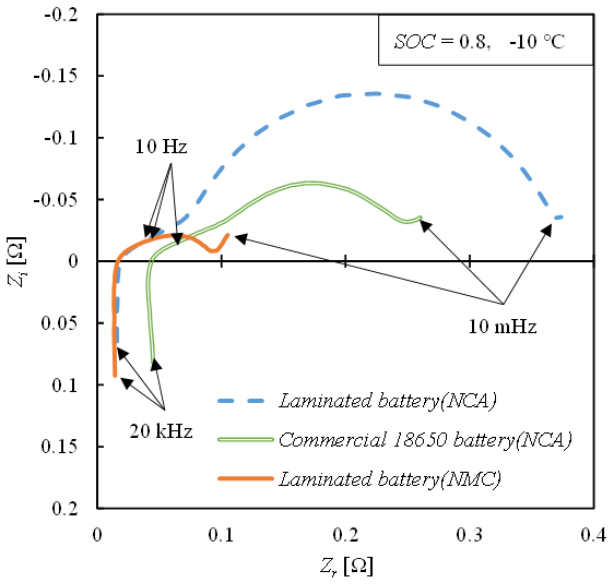


Figure 2. Electrochemical impedances of laminated NCA and NMC batteries alongside a commercial 18650 NCA battery at -10 ℃ and an SOC of 0.8.

Figure 3 depicts the electrochemical impedances of commercial 18650 batteries with NMC cathodes, degraded over varying numbers of degradation cycles, at -10 ℃ and an SOC of 0.8. The figure reveals an increase in the charge transfer resistance on the low-frequency side with advancing degradation cycles, augmenting the corresponding arc's radius. Moreover, the impedance locus on the high-frequency side appears almost unaltered with degradation cycles. The measured results presented in Figures 2 and 3 suggest that the amplification in internal impedance owing to degradation is caused by the cathode.

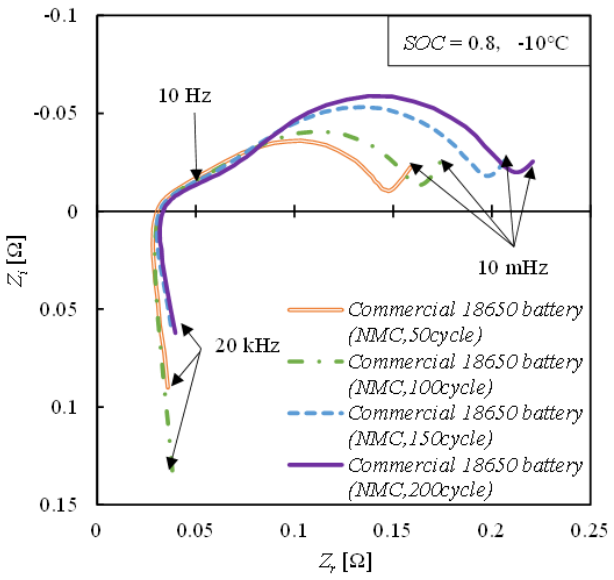


Figure 3. Electrochemical impedances of commercial 18650 batteries with NMC cathodes degraded by different numbers of degradation cycles at -10 ℃ and an SOC of 0.8.

Figure 4 presents the electrochemical impedances of commercial 18650 batteries with an NMC cathode degraded by 150 degradation cycles at disparate temperatures and an SOC of 0.8. The figure underscores that the charge transfer resistance on the low-frequency side intensifies as the temperature decreases.

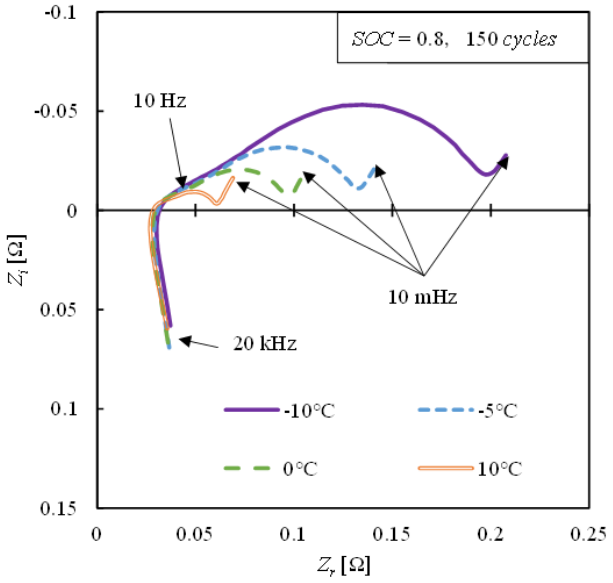


Figure 4. Electrochemical impedances of commercial 18650 batteries with an NMC cathode degraded by 150 degradation cycles at different temperatures and an SOC of 0.8.

Figure 5 displays the electrochemical impedances of commercial 18650 batteries with NMC cathodes degraded by 150 degradation cycles at -10 ℃ temperature and a varying SOC. The figure illustrates a reduction in the charge transfer resistance with an escalating SOC on the low-frequency side, whereas the electrochemical impedance on the high-frequency side remains nearly unchanged. This trend was also the same for degraded batteries with 50 and 100 cycles. However, the measured electrochemical impedance results of commercial 18650 batteries degraded by 200 cycles, as shown in Figure 6, suggest that the charge transfer process on the low-frequency side at a 0.9 SOC is more pronounced than at an SOC of 0.5.

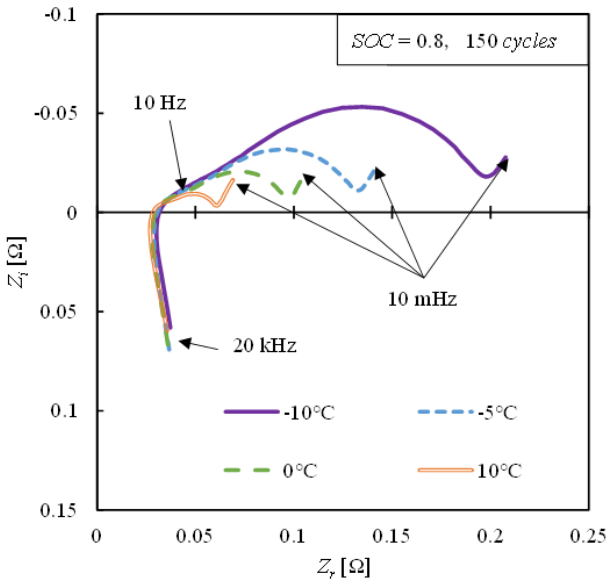


Figure 5. Electrochemical impedances of commercial 18650 batteries with NMC cathodes degraded by 150 degradation cycles at -10 ºC and different SOCs.

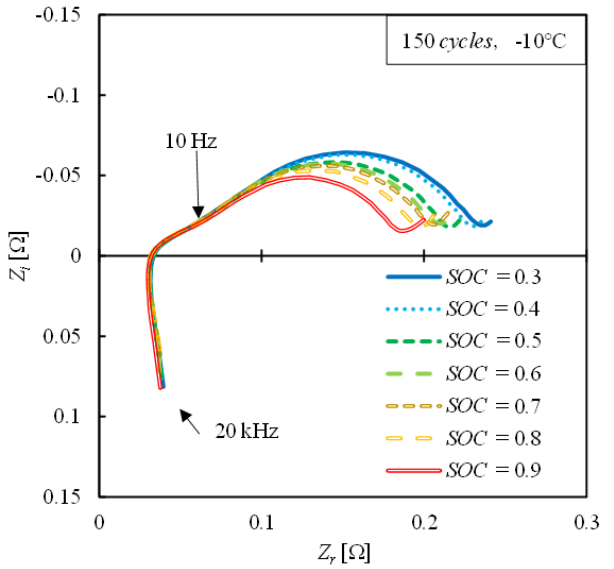


Figure 6. Electrochemical impedances of commercial 18650 batteries with NMC cathodes degraded by 200 degradation cycles at -10 ºC and different SOCs.

## 3. Distribution of relaxation times analysis

Herein, the DRT method was used to dissect the measured electrochemical impedance of the charge transfer process into its elementary processes. We investigated the variations in these processes with respect to the cathode material, cycle degradation and SOC.

### *3.1. Theory of the DRT analysis*

The DRT method facilitated a detailed examination of the measured impedance by separating it further. In this method, the impedance function Z(ω) is considered to comprise an ohmic resistance R0 and an infinite series of RC parallel circuits shown in Figure 7 and is expressed by the following equation:

$$Z(\omega) = R_0 + R_{ct}\int_0^{\infty}\frac{\gamma(\tau)}{1+j\omega\tau}d\tau\,. \tag{1}$$

The term $\gamma(\tau)d\tau/(1+j\omega\tau)$ represents the relative contribution of the RC parallel circuits with a relaxation time of between $\tau$ and $\tau + d\tau$ at the angular frequency $\omega$. R0 is the ohmic resistance, and Rct is the total resistance that exists in the frequency region of the charge transfer process shown in Figure 1. In the numerical computation of the DRT analysis, a finite number of RC parallel circuits are used, and Equation (1) is reformulated as follows:

$$Z(\omega) = R_0 + \sum_{k=1}^{N}\frac{R_k}{1+j\omega\tau_k}\,, \tag{2}$$

where N is the number of RC parallel circuits. The series of $R_k$ is identified from this equation. Then, the relaxation time distribution function $\gamma(\tau)$ can be approximately calculated by considering the following constraint condition:

$$R_{ct}\int_{\tau_{min}}^{\tau_{max}}\gamma(\tau)d\ln\tau = \sum_{k=1}^{N}R_k\,, \tag{3}$$

where $\tau_{max}$ is the maximum time constant of the impedance, and $\tau_{min}$ is the minimum time constant. To depict $\gamma(\tau)$ as a function of the relaxation frequency $f$, we converted the time constant to the relaxation frequency using Equation (4) to obtain the relaxation frequency distribution function $g_R(f)$.

$$\tau = RC = \frac{1}{2\pi f}\,. \tag{4}$$

Prior to conducting the DRT analysis, it is essential to remove the inductive component from the measured electrochemical impedance, as it cannot be accommodated in the DRT analysis. For this purpose, a provisional equivalent circuit model inclusive of $L$ is temporarily applied to the measured impedance data, and the inductance $L$ is identified. Subsequently, the measured imaginary part $Z_i$ is modified using the following equation:

$$Z_i - j\omega L\,. \tag{5}$$

This process ensures an accurate rendition of the impedance data for the ensuing DRT analysis, aiding in a precise interpretation of the charge transfer process and its elementary constituents.

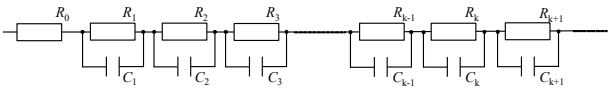


Figure 7. Circuit diagram for DRT analysis.

### *3.2. Results of the DRT method*

Figure 8 displays the DRT results for two laminated batteries with either an NCA or NMC cathode and a commercial cylindrical 18650 battery with an NCA cathode, all measured at -10 ºC and an SOC of 0.8. These DRT results were computed using the measured electrochemical impedance depicted in Figure 2. Four peaks are observed within the frequency range analysed in this study, attributable to the charge transfer processes and the solid electrolyte interphase (SEI) of both electrodes. Table 2 shows the relaxation frequency at which the DRT results take each peak. A distinct peak emerges around 0.3 Hz for both batteries equipped with NCA cathodes, whereas no peak is discernible around this frequency for the battery with an NMC cathode. The frequency range of the charge transfer processes is usually lower than that of the SEI. These suggest that the peak around 0.3 Hz arises from elementary processes associated with the charge transfer process of the cathode. In the two laminated batteries with identical graphite anodes, the peaks occurring at a frequency of around 2 kHz exhibit similar magnitudes. In the commercial 18650 battery, the highest frequency peak is located within the 1-2 kHz range, analogous to those of laminated batteries. This insinuates that the highest frequency peak originates from elementary processes associated with the anode. In general, it is acknowledged that the peak caused by the SEI of the anode resides on the higher-frequency side (Vetter et al., 2005). It is thus inferred that the peak on the high-frequency side results from the SEI of the anode.

Table 2. Relaxation frequency at which DRT results take each peak.

| Battery | Frequency [Hz] | | | |
|---|---|---|---|---|
| | P1 | P2 | P3 | P4 |
| Laminated battery (NCA) | 1860 | 35.0 | 5.24 | 0.26 |
| Commercial 18650 battery (NCA) | 1120 | 42.0 | 4.78 | 0.30 |
| Laminated battery (NMC) | 1620 | 213 | 28.0 | 3.63 |

Comparing the DRT results of laminated and commercial 18650 batteries with NCA cathodes reveals that, despite the significant differences in the impedance measurement outcomes as depicted in Figure 2, each peak emerges within a closely aligned frequency range. Consequently, it is deduced that the DRT analysis yields similar characteristics for batteries with analogous electrode materials.

Figure 9 illustrates the DRT results of commercial cylindrical 18650 batteries with NMC cathodes, degraded by 50, 100, 150, and 200 charge-discharge cycles, at -10 ºC and an SOC of 0.8. Four peaks are evident in each DRT result for batteries with varying cycle degradation, implying that the count of elementary processes remains unaffected by the cycle degradation. It is also discernible that as the cycle degradation advances, the peak at around 1 Hz-presumed to be caused by the charge transfer process of the cathode-amplifies, and its relaxation frequency gravitates towards the lower-frequency side. Contrarily, the peak at the highest frequency, attributed to the SEI of the anode, remains unaltered with cycle degradation. Two peaks within the 10-200 Hz frequency range also transition towards lower frequencies owing to degradation. This analytical observation delineates the inherent resilience of certain electrochemical processes amidst the evolving degradation states, offering a clear understanding of the charge transfer dynamics within these commercial batteries.

Figure 10 illustrates the DRT results of a commercial cylindrical 18650 battery with an NMC cathode, degraded by 150 charge-discharge cycles, across different temperatures while maintaining an SOC of 0.8. These DRT results were derived from the measured electrochemical impedance, as presented in Figure 4. Notably, the peak at around 1 Hz, believed to be induced by the charge transfer process at the cathode, magnifies as the temperature decreases, and its relaxation frequency shifts towards the lower-frequency side. In addition, two peaks within the 10-200 Hz frequency range exhibit a shift towards lower frequencies owing to degradation.

Figure 11 displays the DRT results of a commercial cylindrical 18650 battery with NMC cathode material, degraded by 150 charge-discharge cycles, at -10 ºC and a varying SOC. These DRT results were computed from the measured electrochemical impedance, as depicted in Figure 5. The data reveal minimal change in the relaxation frequency and magnitude of peaks at frequencies above 100 Hz. However, the peaks observed at lower frequencies demonstrate a shift towards the lower-frequency side as the SOC diminishes.

The DRT findings across batteries with diverse levels of degradation cycles suggest that the increase in electrochemical impedance owing to cycle degradation, variations in the SOC and reduction in temperature could be attributed to the charge transfer process of the cathode. Moreover, four principal peaks were discerned in the DRT analysis, unaffected by the type of cathode material and the extent of degradation cycles. Through these analyses, a consistent pattern emerges linking cathode material and electrochemical behaviour, further elucidating the influence of varying operational and material conditions on the impedance characteristics of the batteries.

(a)

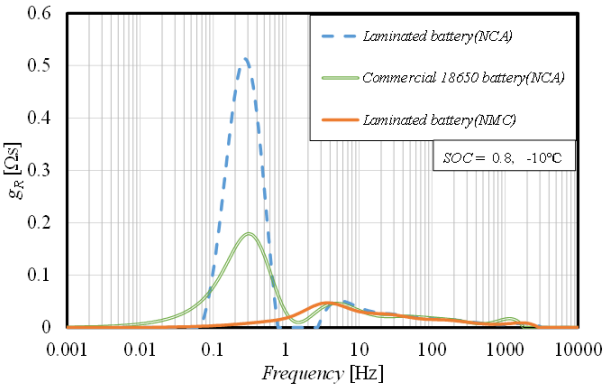


(b)

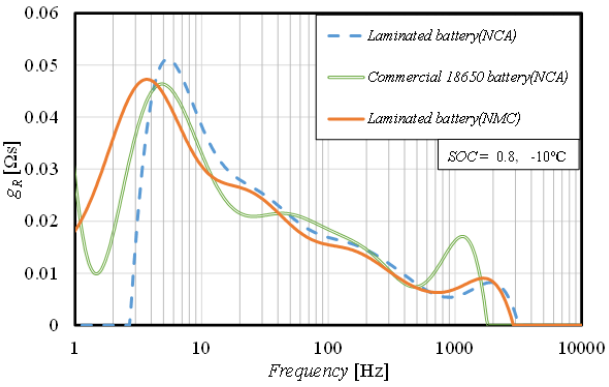


Figure 8. DRT results of laminated NCA and NMC batteries alongside commercial 18650 NCA batteries at -10 ºC and an SOC of 0.8 in: (a) Full frequency range (10 mHz-10 kHz); and (b) Magnification of high frequency range (1 Hz-10 kHz).

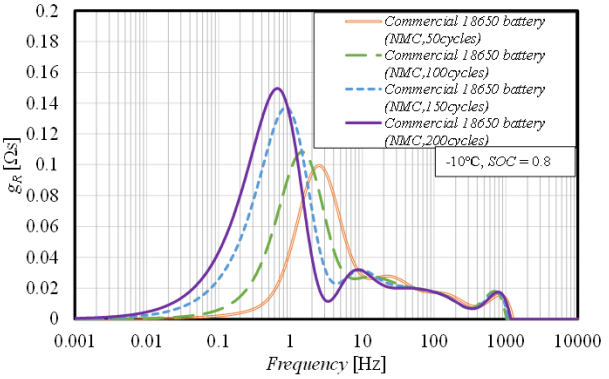


Figure 9. DRT results of commercial 18650 batteries with NMC cathodes degraded by different numbers of degradation cycles at -10 ºC and an SOC of 0.8.

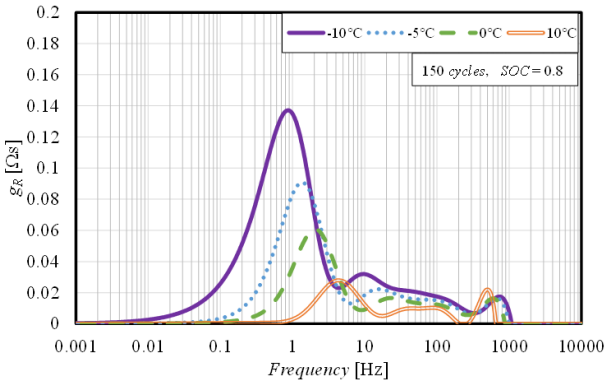


Figure 10. DRT results of commercial 18650 batteries with NMC cathodes degraded by 150 degradation cycles at different temperatures and an SOC of 0.8.

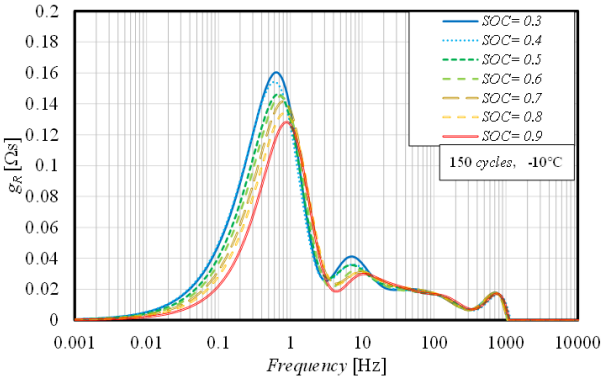


Figure 11. DRT results of commercial 18650 batteries with NMC cathodes degraded by 150 degradation cycles at -10 ºC and different SOCs.

## 4. Conclusions

This study measured the electrochemical impedances of several lithium-ion batteries with varying electrode materials and levels of cycle degradation. The measurements were analysed using the DRT method to investigate the effects of different electrode materials and cycle degradation on the batteries' electrochemical impedance.

The electrochemical impedance of three batteries with distinct cathode materials (laminated batteries with NCA or NMC cathodes and a commercial cylindrical battery with an NCA cathode) was gauged in accordance with EIS. The analysis confirmed the influence of the charge transfer process of the cathode at the frequencies below 10 Hz. Moreover, the separation of electrochemical impedance's elementary processes using the DRT method suggested the presence of four main processes, as evidenced by the four peaks observed in all the types of test batteries.

The measurements of the batteries subjected to varying levels of cyclic degradation revealed an increase in

the charge transfer resistance in the lower-frequency region (below approximately 10 Hz) as the degradation progressed. However, in the frequency region above approximately 10 Hz, the electrochemical impedance remained relatively unchanged with degradation. It was also observed that the charge transfer resistance within the frequency region below 10 Hz escalated with decreasing temperature and SOC. In addition, the DRT analysis unveiled a consistent occurrence of four peaks in the DRT under low-temperature conditions across all the battery types, irrespective of the degradation level. The DRT peak at the lowest frequency exhibited the most notable change: as the temperature decreased, the relaxation frequency shifted towards the lower-frequency side, and the peak heightened. Similarly, under low-temperature and SOC conditions, the relaxation frequency of the same peak shifted towards the lower-frequency side, and then, the peak escalated. These results underscore that the most significant impact of degradation manifests itself as an increase in the cathode's charge transfer resistance, particularly under low-temperature and low-SOC conditions.

## Notes on contributors

**Mr Sohei Tomita** received his B.E. degree from The University of Shiga Prefecture, Japan, in 2022. He is presently a graduate student with the University of Shiga Prefecture, Japan. His research interests include lithium-ion batteries.

**Mr Daiki Kawaguchi** is a graduate student at the Graduate School of Engineering, The University of Shiga Prefecture. His research interests include lithium-ion batteries.

**Dr Satoshi Hirayama** received a Ph.D. degree in Engineering from The University of Tsukuba in 2015, and is presently a lecturer at The University of Shiga Prefecture, Japan. His research interests include lithium-ion batteries, arc interruption phenomena, and electric power apparatus.

**Prof Yoshitaka Inui** is permanently working at The University of Shiga Prefecture as a Professor. His research interests include electric energy systems, power electronics, lithium-ion batteries, photovoltaic systems, etc. He is a member of IEE Japan.

## References


[1] Choi W, Shin HC, Kim JM, Choi JY, Yoon WS (2020), Modeling and Applications of Electrochemical Impedance Spectroscopy (EIS) for Lithium-ion Batteries. *J. Electrochem. Sci. Technol*, 11(1), p1-13.

[2] Illig J, Ender M, Chrobak T, Schmidt JP, Klotz D and Ivers-Tiffée E (2012). Separation of Charge Transfer and Contact Resistance in LiFePO4-Cathodes by Impedance Modeling. *Journal of the Electrochemical Society*, 159, A952-960.

[3] Jow TR, Delp SA, Allen JL, Jones JP, Smart CM (2018), Factors Limiting Li+ Charge Transfer Kinetics in Li-Ion Batteries. *Journal of The Electrochemical Society*, 165(2), A361-367.

[4] Li T, Yuan XZ, Zhang L, Song D, Shi K, and Bock C (2020). Degradation Mechanisms and Mitigation Strategies of Nickel-Rich NMC-Based Lithium-Ion Batteries. *Electrochemical Energy Reviews*, 3, pp. 43-80.

[5] Ohzuku T and Brodd RJ (2007). An Overview of Positive-electrode Materials for Advanced Lithium-ion Batteries. *J. Power Sources*, 174(2), pp. 449-456.

[6] Okada S, Yoshitake S, Tominaga Y and Anekawa A (2013). Development of Lithium-ion Battery Deterioration Diagnosis Technology. *Yokogawa Technical Report English Edition*, 56 (2), pp.75-78.

[7] Sun HH, Ryu HH, Kim UH, Weeks JA, Heller A, Sun YK and Mullins CB (2020). Beyond Doping and Coating: Prospective Strategies for Stable High-Capacity Layered Ni-Rich Cathodes. *ACS Energy Lett*, 5 (4), pp.1136-1146.

[8] Vetter J, Novák P, Wagner RM, Veit C, Möller KC, Besenhard JO, Winter M,Wohlfahrt-Mehrens M, Vogler C and Hammouche A (2005). Ageing mechanisms in lithium-ion batteries. *Journal of Power Sources*, 147(1-2), pp. 269-281.

[9] Zeng X, Zhan C, Lu J and Amine K (2018). Stabilization of a High-Capacity and High-Power Nickel-Based Cathode for Li-Ion Batteries. *Chem*, 4 (4), pp.690-704.